Low-temperature in-situ combustion of light oil*

A.A. Mailybaev†, J. Bruining‡, D. Marchesin§

1 Introduction

Recovery percentages from oil reservoirs range from 5% for difficult oil to 50% for light oil in highly permeable sandstone reservoirs. Other reservoirs contain oil that is too difficult to produce with conventional means. Part of this oil can be recovered using the methods of enhanced oil recovery (EOR).

One of the methods to enhance the recovery uses air injection leading to oil combustion. Conventional oil combustion can be considered as an in-situ heat generation process and its purpose is lowering the viscosity of oil. Two major types of oxidation processes are identified. The high temperature oxidation (HTO) process includes coke formation and its subsequent oxidation at temperatures above 350℃. Due to a high reaction rate, the HTO reactions occur in thin reaction zones. In the low temperature oxidation (LTO) process hydrocarbons are gradually oxidized through the formation of ketones, alcohols, aldehydes and acids at temperatures less than 300℃. As LTO only involves some 25 % [4] of the possible sites that can react with oxygen, also the reaction heat per volume of fuel is roughly 25 % and consequently the temperature in the LTO reaction zone is very low. The order of magnitude of the reaction rates is comparable with the reaction rates found for HTO. However, since the oxygen concentration is much less than the fuel concentration in terms of moles/m^3, the oxygen consumption can occur within meters at the highest temperatures (300℃).

In this work we examine a very simplified model for LTO, which is probably more suitable to describe clean up of gasoline (represented as heptane) spilled in dry porous rock. In this model a single pseudo-component liquid fuel is considered, which is characterized by an average boiling temperature, density, viscosity etc. Application of this theory to in-situ combustion is limited by the fact that oil contains heavy components which do not vaporize and lead to the change of solution. Our theory, however, provides understanding of interaction of three physical processes: LTO, vaporization and permeability effects. The main result is the resonance condition that determines combustion wave parameters. This condition appears to be generic and can be used in different models.

*This work was supported in part by: CNPq under Grants 304168/2006-8, 472067/2006-0, 474121/2008-9, FAPERJ under Grants E-26/152.525/2006, E-26/102.723/2008, E-26/112.220/2008, E-26/110.310/2007, E-26/112.112/2008.

†Corresponding author: Institute of Mechanics, Moscow State University, Michurinsky pr. 1, 119192 Moscow, Russia. E-mail: mailybaev@imec.msu.ru

‡TU Delft, Civil Engineering and Geosciences, Stevinweg 1, 2628 CE Delft, The Netherlands. E-mail: J.Bruining@tudelft.nl

§Instituto Nacional de Matemtica Pura e Aplicada, Estrada Dona Castorina 110, 22460-320 Rio de Janeiro, RJ, Brazil. E-mail: marchesi@impa.br

2 Model

We consider flows possessing a combustion front when a gaseous oxidizer (air) is injected into the porous medium, a rock cylinder thermally insulated preventing lateral heat losses and filled with light or medium viscosity oil. When oxygen reacts with hydrocarbons at low temperatures, a series of reactions occur that will convert a part of hydrocarbons to oxygenated hydrocarbons and gaseous product (water, carbon dioxide etc.). The oxygenated hydrocarbons are compounds like ketones, alcohols, aldehydes and acids. This low temperature oxidation (LTO) reaction is modelled as

$$(\text{oil}) + \text{O}_2 \rightarrow (\text{oxygenated oil}) + \nu_g\,(\text{gaseous products}), \tag{1}$$

i.e., one mole of oxygen reacts with some amount of oil leaving oxygenated oil together with ν_g moles of gaseous products.

Assuming that chains are not broken, we ignore any viscosity- and molar mass changes of the oil. The boiling points will be elevated, but to keep the model tractable we will ignore this fact and assume an average boiling point. As a consequence of this assumption, all oil upstream of the combustion front will be vaporized as we will see in the analysis. We consider situations at low temperatures (small reaction rates) so that only few carbons in each hydrocarbon molecule get oxygenated, so we can disregard the difference between oxygenated and initial hydrocarbons and consider a single oil pseudo-component. We assume that the original oil contains so little heavy hydrocarbons that we can ignore coke formation, so that high temperature oxidation is not possible. The concentration of water initially present in the reservoir or condensed from the vapor generated in the LTO reaction is disregarded. Actually, our model could easily be modified to deal with immobile (connate) water.

We study a simplified model, in which hydrocarbons act as a single pseudo-component that can be both in the gas and in the liquid phase. The average oil molar weight is denoted by M_o [kg/mole]. The saturation of the liquid oil will be denoted by S (a fraction of pore volume occupied by liquid oil). The saturation of gas is, therefore, equal to $1-S$. In the gas phase, we distinguish between the molar fraction of gaseous oil X, of oxygen Y and of the remaining gas fraction $Z = 1 - X - Y$ that consists of reaction products and inert components of the injected gas. Neglecting gas mass diffusion and capillarity effects, the balance equations for liquid oil and gas components (gaseous oil, oxygen, and remaining gaseous components) are

$$\frac{\partial}{\partial t}\varphi\rho_o S + \frac{\partial}{\partial x}\rho_o u f_o = -W_v, \tag{2}$$

$$\frac{\partial}{\partial t}\varphi\rho_g X(1-S) + \frac{\partial}{\partial x}\rho_g u f_g X = W_v, \tag{3}$$

$$\frac{\partial}{\partial t}\varphi\rho_g Y(1-S) + \frac{\partial}{\partial x}\rho_g u f_g Y = -W_c, \tag{4}$$

$$\frac{\partial}{\partial t}\varphi\rho_g Z(1-S) + \frac{\partial}{\partial x}\rho_g u f_g Z = \nu_g W_c. \tag{5}$$

The sum of (3)–(5) together with the relation $X+Y+Z=1$ yield the total gaseous components balance law

$$\frac{\partial}{\partial t}\varphi\rho_g(1-S) + \frac{\partial}{\partial x}\rho_g u f_g = (\nu_g - 1)W_c + W_v. \tag{6}$$

In the equations, W_v [mole/m^{3}s] is the vaporization rate of hydrocarbons, W_c [mole/m^{3}s] is the consumption rate of oxygen in the LTO reaction; according to (1) $\nu_g W_c$ is the generation rate of gaseous products. Also, φ is the rock porosity, ρ_o [mole/m^3] is the molar density of the liquid oil evaluated in terms of average molar weight M_o (the conventional mass density is, therefore,

$M_o\rho_o$), u [m/s] is the total seepage velocity, and

$$\rho_g = P_{tot}/RT \tag{7}$$

is the molar density of gas at the prevailing pressure P_{tot} [Pa] and temperature T [K]. Pressure variations are assumed to be small, so we take $P_{tot} = const$. The fractional flow functions are

$$f_o = \frac{k_o/\mu_o}{k_g/\mu_g + k_o/\mu_o}, \quad f_g = \frac{k_g/\mu_g}{k_g/\mu_g + k_o/\mu_o}, \tag{8}$$

where $\mu_o(T)$, $\mu_g(T)$ [kg/m s] are the oil and gas phase viscosities. We assume that the relative permeability functions $k_o(S)$ and $k_g(S)$ are positive with $k_o(0) = k_o'(0) = 0$ and $k_g(1) = k_g'(1) = 0$. For example, in the quadratic Corey model one can use $k_o = S^2$, $k_g = (1-S)^2$.

Assuming that the temperature of solid rock, liquid oil and gas are equal and neglecting heat losses, we write the heat transport equation as

$$\frac{\partial}{\partial t}(C_m + \varphi c_o\rho_o S + \varphi c_g\rho_g(1-S))\Delta T + \frac{\partial}{\partial x}(c_g\rho_g u f_g + c_o\rho_o u f_o)\Delta T = Q_c W_c - Q_v W_v. \tag{9}$$

Here $\Delta T = T - T_{res}$ with the reservoir temperature T_{res}, C_m [J/m^{3}K] is constant the heat capacity of the porous rock, c_o [J/mole K] is the heat capacity of liquid oil per average mole M_o taken as a constant for simplicity, and $c_g \approx 3.5R$ [J/mole K] is the approximate gas heat capacity, ignoring small variations of heat capacity among different gas components. The positive heats (enthalpies) Q_c [J/mole of O_2] and Q_v [J/mole of oil] correspond to the LTO reaction and vaporization of light oil evaluated at the reservoir temperature T_{res}, taken per mole of oxygen and oil, respectively. We neglected heat losses and diffusion effects. Conditions justifying these simplifications will be given in a separate section.

The vaporization rate W_v vanishes when liquid oil is in thermodynamic equilibrium with its gaseous phase. The gaseous oil partial pressure equals $P_o = XP_{tot}$. In thermodynamic equilibrium, we have

$$X_{eq} = \frac{P_o}{P_{tot}} = \frac{P_{atm}}{P_{tot}} \exp\left(-\frac{Q_v}{R}\left(\frac{1}{T} - \frac{1}{T_{bn}}\right)\right), \tag{10}$$

where T_{bn} [K] is the normal boiling point. Taking $P_o = P_{tot}$ in (10), one recovers the actual boiling temperature $T = T_b$ at pressure P_{tot}. For the temperatures under consideration, which do not exceed the boiling temperature, the vaporization process is much faster than the LTO reaction, $|W_v| \gg W_c$. In this case, as we will see later, the specific forms of combustion rates W_c and W_v are not important for determining macroscopic solution parameters. They affect only the width of the LTO wave and its internal structure.

All the coefficients in the equations (C_m, c_g, ρ_o, etc.) are assumed to be constant, if not stated otherwise. The air injection data are characterized by the Darcy velocity u_{inj} and oxygen fraction Y_{inj}.

2.1 Dimensionless equations

The governing equations are non-dimensionalized by introducing dimensionless dependent and independent variables as ratios of dimensional quantities and reference quantities:

$$\tilde{t} = \frac{v^* t}{x^*}, \quad \tilde{x} = \frac{x}{x^*}, \quad \theta = \frac{T - T_{res}}{T^*}, \quad m = \frac{\rho_g u f_g}{\rho_g^* u_{inj}}, \tag{11}$$

where

$$\rho_g^* = \frac{P_{tot}}{RT_{res}}, \; x^* = \frac{Y_{inj}\rho_g^* u_{inj}}{W_c^*}, \; v^* = \frac{u_{inj}}{\varphi}\left(\frac{\mu_g}{\mu_o}\right)_{T=T_{res}}, \; T^* = T_b - T_{res}, \tag{12}$$

and T_b is the boiling temperature at the pressure P_{tot}, and W_c^* is the characteristic value of the reaction rate at reservoir temperature (see Eq. (53)). The dimensionless quantities θ and m describe the temperature and gas flux, respectively. The length scale x^* is the ratio of oxygen flux injected and oxygen consumption in the LTO reaction, and v^* is the reference oil speed when gas is injected. Thus, x^* and v^* are chosen as reference quantities for the length and speed of the LTO wave. The following analysis is carried out under the assumption that x^* is much smaller than the overall problem scale, i.e., distance between injection and producing wells.

Using (8), (11), (12) and omitting the tildes in the dimensionless quantities, equations (9), (2)–(4) and (6) are written in dimensionless form as

$$\frac{\partial(1+aS+\varepsilon v_T(1-S)\theta_0/(\theta_0+\theta))\theta}{\partial t}+\frac{\partial(v_T\theta m+a\theta F)}{\partial x} = q(w_c-rw_v), \tag{13}$$

$$\frac{\partial S}{\partial t}+\frac{\partial F}{\partial x} = -bw_v, \tag{14}$$

$$\varepsilon\frac{\partial}{\partial t}\frac{\theta_0(1-S)X}{\theta_0+\theta}+\frac{\partial Xm}{\partial x} = w_v, \tag{15}$$

$$\varepsilon\frac{\partial}{\partial t}\frac{\theta_0(1-S)Y}{\theta_0+\theta}+\frac{\partial Ym}{\partial x} = -w_c, \tag{16}$$

$$\varepsilon\frac{\partial}{\partial t}\frac{\theta_0(1-S)}{\theta_0+\theta}+\frac{\partial m}{\partial x} = (\nu_g-1)w_c+w_v, \tag{17}$$

with the dimensionless quantities

$$\varepsilon=\left(\frac{\mu_g}{\mu_o}\right)_{T=T_{res}},\ a=\frac{\varphi c_o\rho_o}{C_m},\ b=\frac{\rho_g^*}{\varepsilon\rho_o},\ r=\frac{Q_v}{Q_c},\ q=\frac{\varphi\rho_g^*Q_c}{\varepsilon C_mT^*},$$
$$v_T=\frac{\varphi c_g\rho_g^*}{\varepsilon C_m},\ h_v=\frac{Q_v}{RT^*},\ \theta_0=\frac{T_{res}}{T^*} \tag{18}$$

and functions

$$F(\theta,S,m)=\eta\psi m,\ \eta(\theta)=\frac{(\theta_0+\theta)\mu_g}{\varepsilon\theta_0\mu_o},\ \psi(S)=\frac{k_o}{k_g}. \tag{19}$$

Note that $\varepsilon\sim10^{-2}\ll1$, due to the small ratio between gas and oil viscosities. The quantities $\eta(\theta)$ and $\psi(S)$ are increasing functions of their arguments with the properties

$$\eta(0)=1,\quad \psi(0)=\psi'(0)=0,\quad \psi(1)=\infty. \tag{20}$$

The dimensionless combustion and vaporization rates are $w_{c,v}=x^*W_{c,v}/(\rho_g^*u_{inj})$. Using (10), we get

$$X_{eq}(\theta)=\exp\left(\frac{h_v}{\theta_0+1}-\frac{h_v}{\theta_0+\theta}\right). \tag{21}$$

The condition at $x=0$ (injection well) is $m=1$, $\theta=S=X=0$, $Y=Y_{inj}$. The initial reservoir state is $\theta=0$, $S=1$, $X=X_{eq}(0)$, $Y=0$.

3 Thermal and saturation waves

The LTO reaction with injected oxygen leads to complete removal of liquid oil. Behind the LTO zone, there is no oil, $S=X=0$, and the gas flux is constant and equal to its value $m=1$ at the

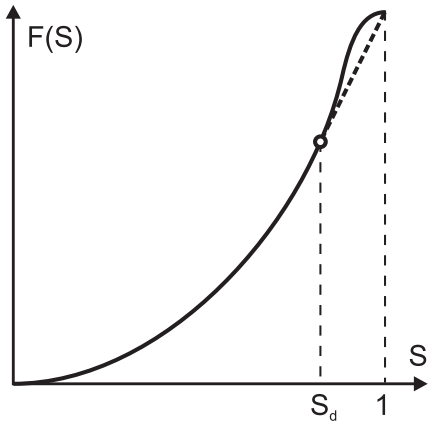

Figure 1: The oil flux function and saturation wave structure. Rarefaction wave for saturations $S < S_d$ followed by a shock from S_d to $S = 1$

injection point. In the absence of oil, the reaction and vaporization rates and the terms related to the heat accumulated and transported by oil vanish and (13) becomes

$$\frac{\partial \theta}{\partial t} + v_T \frac{\partial \theta}{\partial x} = 0, \tag{22}$$

where we used $F = 0$ (zero oil flux) and neglected the small ε-term related to the heat accumulated by the gas. This equation possesses a wave solution $\theta = \theta_r H(v_T t)$, where $H(\cdot)$ is the unit step function. This wave moves with speed v_T, and the temperature changes from θ_r ahead of the wave to the temperature of the injected gas $\theta = 0$. If thermal conduction is taken into account, the wave profile becomes smooth and its width increases in time proportionally to $\sqrt{t}$, see, e.g., [3].

Ahead of the LTO zone, the gas moves through the porous medium containing oil at the initial reservoir temperature $\theta = 0$. This gas contains the equilibrium oil vapor fraction $X_0 = X_{eq}(0)$ and no oxygen $Y = 0$, so that the vaporization and reaction rates vanish, $w_v = w_c = 0$. The change of oil saturation is governed by equation (14), which takes the standard fractional flow form

$$\frac{\partial S}{\partial t} + \frac{\partial \tilde{u} f_o}{\partial x} = 0, \tag{23}$$

where $\tilde{u} = u/u_{inj}$ is the dimensionless total seepage velocity, which is constant, and the oil fractional flow function f_o is evaluated at the reservoir temperature $\theta = 0$. The function $f_o(S)$ has typically the S-shaped form, see Fig. 1. Using (8), (18), (19), one can check that $f_o(S) = \psi(S)/(1 + \varepsilon\psi(S))$. When ε is small, the inflection point is close to $S = 1$. For example, for the quadratic model with $\psi = S^2/(1 - S)^2$, the inflection point is found at $S \approx 1 - \sqrt{\varepsilon/3}$.

Equation (23) has a well-known self-similar solution $S = S(x/t)$ representing a saturation wave. It has a smooth part (rarefaction) satisfying the equation

$$x/t = \tilde{u} f_o'(S) \tag{24}$$

followed by a discontinuity (shock) from S_d to $S = 1$ propagating with speed $x/t = v_d$, see Fig. 1. The rarefaction wave corresponds to a concave part of $f_o(S)$, where $f_o'(S)$ increases. The shock wave state and speed are determined by the conditions

$$v_d = \tilde{u} f_o'(S_d) = \tilde{u}\, \frac{f_o(1) - f_o(S_d)}{1 - S_d}. \tag{25}$$

For the quadratic model with $\psi = S^2/(1 - S)^2$ and small ε, one obtains $S_d \approx 1 - \sqrt{\varepsilon}$ and $v_d \approx (\tilde{u}/2)\varepsilon^{-3/2}$. When all states in the saturation wave belong to the convex region of $f_o(S)$

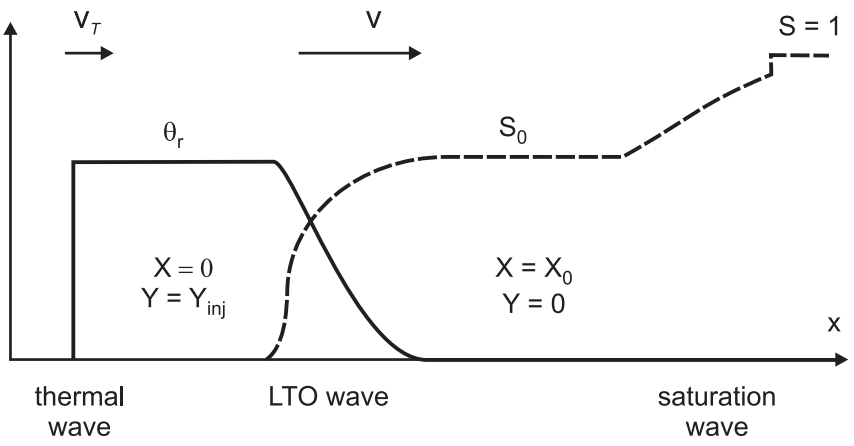

Figure 2: Wave sequence for the low-temperature combustion process.

(i.e., to the right of the inflection point), the wave is a single discontinuity from a point S_0 to $S = 1$ propagating with speed

$$v_d = \tilde{u}\,\frac{f_o(1) - f_o(S_0)}{1 - S_0}. \tag{26}$$

The gas flux in the saturation wave can be found using (8), (11), (18), (19) as

$$m = \tilde{u} f_g = \frac{\tilde{u}}{1 + \varepsilon\psi(S)}. \tag{27}$$

Thus, the total seepage velocity $\tilde{u}$ can be found if one knows the gas flux m_0 and oil saturation S_0 upstream of the saturation wave.

4 Low-temperature oxidation wave

The LTO wave is the wave where oxygen reacts with liquid oil. We make the assumption, confirmed by the ensuing analysis, that the LTO wave is a traveling wave with speed v faster than the thermal wave, but slower than the saturation wave, see Fig. 2. The temperature upstream of the LTO wave is denoted by θ_r. The oil saturation and the gas flux downstream of the LTO wave are denoted by S_0 and m_0. Thus, our assumptions about the wave sequence can be summarized as

$$v_T < v < \min\{(\partial F/\partial S)_0,\, v_d\}. \tag{28}$$

Here the derivative $(\partial F/\partial S)_0$ is evaluated at $\theta = 0$, S_0, m_0, so that the right-hand side of (28) gives the minimal speed in the saturation wave, as shown in the previous section.

The LTO reaction stops behind the wave due to lack of oil, and the gas composition corresponds to the injected gas. Thus, behind the LTO wave, we have a constant state with

$$\theta = \theta_r, \quad S = 0, \quad X = 0, \quad Y = Y_{inj}, \quad m = 1. \tag{29}$$

Ahead of the LTO wave, the reaction stops due to lack of oxygen, and the temperature is equal to the reservoir temperature. The corresponding constant state is

$$\theta = 0, \quad S = S_0, \quad X = X_0, \quad Y = 0, \quad m = m_0. \tag{30}$$

4.1 LTO wave profile equations

In a traveling wave, all variables depend on a single traveling coordinate $\xi = x - vt$. To simplify the formulae, we neglect small ε-terms on the left-hand sides (corresponding to heat capacity and gas mass in accumulation terms), and write equations (13)–(17) as

$$-v\frac{\partial(1+aS)\theta}{\partial\xi} + \frac{\partial(v_T\theta m + a\theta F)}{\partial\xi} = -q\left(\frac{\partial Ym}{\partial\xi} + r\frac{\partial Xm}{\partial\xi}\right), \tag{31}$$

$$-v\frac{\partial S}{\partial\xi} + \frac{\partial F}{\partial\xi} = -b\frac{\partial Xm}{\partial\xi}, \tag{32}$$

$$\frac{\partial Xm}{\partial\xi} = w_v, \tag{33}$$

$$\frac{\partial Ym}{\partial\xi} = -w_c, \tag{34}$$

$$\frac{\partial m}{\partial\xi} = -(\nu_g - 1)\frac{\partial Ym}{\partial\xi} + \frac{\partial Xm}{\partial\xi}, \tag{35}$$

where the reaction rates in the first two and last equations were replaced using (33), (34). Using the conditions (29) behind the wave and $\psi(0) = 0$ (see Eq. (19)), we integrate (31), (32), (35) as

$$-v(1+aS)\theta + v_T m\theta + a\theta F = -q(Y + rX)m + qY_{inj} + (v_T - v)\theta_r. \tag{36}$$

$$-vS + F = -bXm. \tag{37}$$

$$m = \frac{1 + (\nu_g - 1)Y_{inj}}{1 + (\nu_g - 1)Y - X}. \tag{38}$$

Expressing F from (37) and substituting into (36) yields

$$-v\theta + v_T m\theta = -qYm - (qr - ab\theta)Xm + qY_{inj} - (v - v_T)\theta_r. \tag{39}$$

In order to facilitate the analysis of the LTO wave profile, additional simplifications can be done. We neglect the small terms $(\nu_g - 1)Y \sim 0.1$ in (38) and all the terms with the factors $r \sim 0.1$, $v_T \sim 0.1qY_{inj}$ and $ab \sim 0.1q$ in (39). The latter simplifications use the fact that the combustion heat Q_c is much larger than the oil evaporation heat Q_v or the oil and gas sensible heats c_oT^* and c_gT^*, as one can see using (18). The resulting simplified equations obtained from (37), (38) and (39) are

$$vS - F(\theta, S, m) - bXm = 0, \quad m = 1/(1 - X), \tag{40}$$

$$-v\theta = -qYm + qY_{inj} - v\theta_r. \tag{41}$$

Since ahead of the wave $\theta = Y = 0$, equation (41) yields

$$\theta = qYm/v, \tag{42}$$

where we expressed

$$\theta_r = qY_{inj}/v. \tag{43}$$

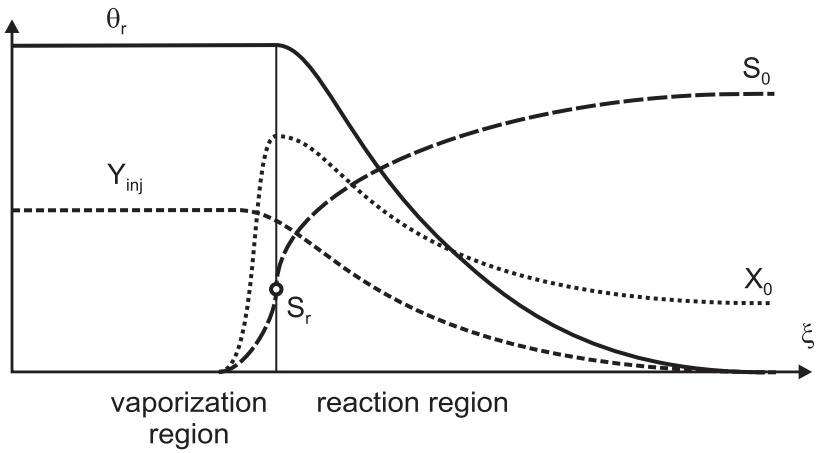

Figure 3: Structure of the low-temperature oxidation wave. Change in temperature θ, liquid oil saturation S, oxygen fraction Y and oil fraction X in the gas. One region is dominated by vaporization and the other by LTO reaction (with slow condensation). The spatial scale is schematic, since the reaction region is usually several orders wider than the vaporization region.

4.2 LTO wave structure

Since we have assumed that vaporization is a much faster process than combustion, the LTO wave can be subdivided into two regions corresponding to vaporization and LTO reaction processes. The gas enters in contact with the liquid oil in a thin vaporization region upstream of the wave. Here the gaseous oil fraction increases rapidly from $X = 0$ in the injected air to its equilibrium value $X_{eq}(\theta)$, see Fig. 3. The second much wider reaction region is where the LTO reaction occurs. In the analysis of these regions we will use the fact that $F(\theta, S, m)$ is an increasing function of both θ and m, and $\partial F/\partial S = 0$ for $S = 0$.

In the vaporization region, the reaction rate w_c can be neglected. The oxygen flux determined by (34) does not change and is equal to its value upstream $Ym = Y_{inj}$. The temperature $\theta = qY_{inj}/v$ given by (42) is also constant. The gas flux $m = 1/(1-X)$ is an increasing function of X. The relation between S and X is determined by expression (40), whose differentiation yields

$$\frac{dX}{dS} = \left(v - \frac{\partial F}{\partial S}\right)\left(\frac{\partial F}{\partial m}\frac{dm}{dX} + bm + bX\frac{dm}{dX}\right)^{-1}. \tag{44}$$

The denominator in the right-hand side is positive, since $\partial F/\partial m$ and dm/dX are both positive. Thus, X increases with S when

$$v > \partial F/\partial S. \tag{45}$$

In particular, this condition is satisfied at the constant state behind the LTO wave, where $S = 0$ and $\partial F/\partial S = 0$. The increase of X is bounded by a resonance point, where the derivative (44) vanishes,

$$v = (\partial F/\partial S)_r. \tag{46}$$

The subscript r denotes the value at the resonance point θ_r, S_r, $m_r = 1/(1-X_r)$. Since X must increase in the vaporization region, the solution cannot be continued through the resonance point.

In the reaction region, the oil vapor fraction can be taken equal to its equilibrium value $X = X_{eq}(\theta)$. Since the temperature decreases downstream, the gaseous oil condenses in this region. Due to the LTO reaction, the oxygen flux $m_Y := Ym$ governed by (34) decreases monotonically from the value Y_{inj} upstream to zero downstream. Using (42) one can see that

θ, $X = X_{eq}(\theta)$ and $m = 1/(1-X)$ are increasing functions of m_Y. The relation between S and m_Y is determined by expression (40), whose differentiation yields

$$\frac{dm_Y}{dS} = \left(v - \frac{\partial F}{\partial S}\right)\left(\frac{\partial F}{\partial \theta}\frac{d\theta}{dm_Y} + \frac{\partial F}{\partial m}\frac{dm}{dm_Y} + b\frac{d(X_{eq}(\theta)m)}{dm_Y}\right)^{-1}. \tag{47}$$

The denominator on the right-hand side is positive. Thus, m_Y increases when S decreases provided that

$$v < \partial F/\partial S. \tag{48}$$

In particular, this condition is satisfied at the constant state downstream as is assumed in (28). The value of m_Y is bounded by a resonance point (46), where the derivative (47) vanishes. Since the oxygen flux m_Y changes monotonically in the reaction region, the solution cannot be continued through the resonance point in this region.

We see that the inequalities (45) and (48) have opposite signs in the vaporization and reaction regions. Thus, these regions can be connected only at the resonance point determined by equation (46). Substituting v from (46) with $F = \eta(\theta)\psi(S)m$ into (40), (42) we obtain extra conditions at the resonance point as

$$S_r - \frac{\psi(S_r)}{\psi'(S_r)} = \frac{b\theta_r X_{eq}(\theta_r)}{qY_{inj}(1 - X_{eq}(\theta_r))}, \quad \psi'(S_r) = \frac{qY_{inj}(1 - X_{eq}(\theta_r))}{\theta_r \eta(\theta_r)}, \tag{49}$$

where we used the second expression on the right-hand side of the first expression together with the relations $Ym = Y_{inj}$ in the vaporization region and $X_r = X_{eq}(\theta_r)$ in the reaction region evaluated at the resonance point.

It is easy to see that equations (49) determine the resonance point uniquely in the case when both $\psi'(S)$ and $S - \psi(S)/\psi'(S)$ are positive increasing functions of S vanishing at $S = 0$. This follows from the observation that the left-hand sides of the first two equations in (49) are increasing functions of S_r, while the right-hand sides are increasing and decreasing functions of θ_r, respectively. In particular, this is the case for the quadratic permeability model, for which $\psi(S) = S^2/(1-S)^2$.

With the LTO wave speed given by (46), the relation among all dependent variables θ, S, X, Y, m in both regions are determined as described above. Recall that when solving the first equation in (40) for S, one must choose the solution branch passing through the resonance value S_r and satisfying condition (45) in the vaporization region and (48) in the reaction region. The dependence of the variables on the spatial moving coordinate ξ can be found by numerical integration of equation (33) in the vaporization region and equation (34) in the reaction region.

4.3 LTO wave parameters

We see that the speed (46) and the states ahead and behind the LTO wave are determined by the resonance point of the wave profile. The temperatures θ_r behind the LTO wave and at the resonance point are the same. The constant state ahead of the LTO wave is characterized by $\theta = 0$, $X_0 = X_{eq}(0)$ and $m_0 = 1/(1 - X_0)$. The equation for the corresponding oil saturation S_0 is found by taking $F = \psi(S_0)m_0$ in (40) as

$$vS_0 - \psi(S_0)m_0 = bX_0 m_0, \tag{50}$$

where one must chose S_0 on the solution branch in the reaction region as described above.

One can see from (43), (49), (50) that the quantities in the LTO wave are determined by the dimensionless parameters b, q, Y_{inj}, and the function $\eta(\theta)$, $\psi(S)$, $X_{eq}(\theta)$ defined in (18), (21). These quantities are independent on the air injection velocity u_{inj}. The latter influences only the spatial and velocity scales in (12), which are proportional to u_{inj}.

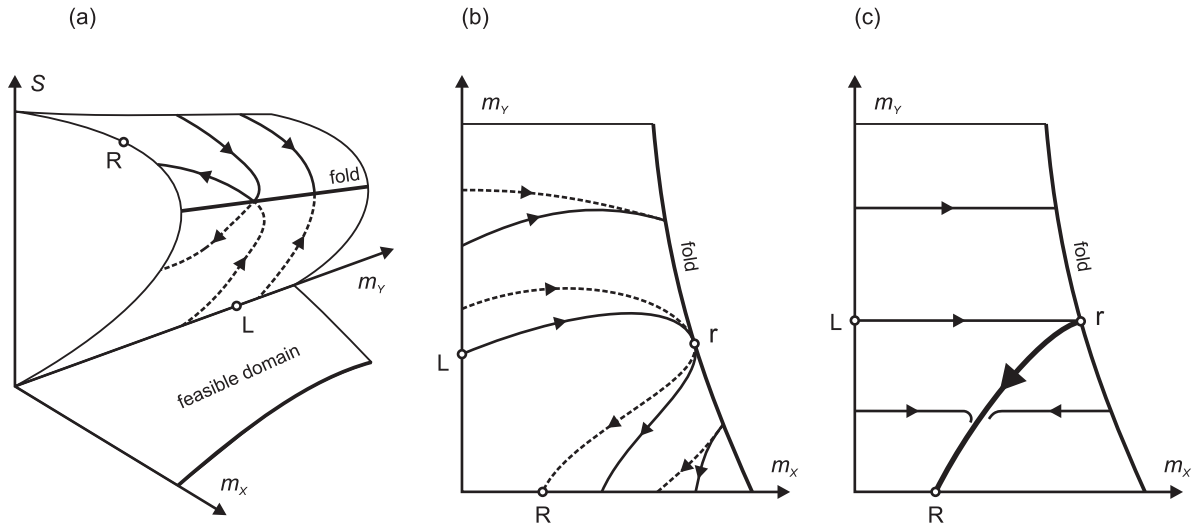

Figure 4: Geometric explanation of the LTO wave resonance condition. (a) A fold singularity of the S- surface and the feasible domain. (b) Integral curves on the plane of gaseous oil and oxygen fluxes. Solid and dotted lines correspond to the upper and lower parts of the S-surface, respectively. (c) Integral curves in the case of high vaporization rate.

Let us verify the initial assumptions (28). Using (43), we find $v = qY_{inj}/\theta_r$ with $\theta_r < 1$. As was mentioned above, $v_T \sim 0.1qY_{inj}$, so that the first condition in (28) is valid. The second condition $v < (\partial F/\partial S)_0$ is satisfied by construction of the LTO wave profile in the reaction region, where (48) holds. The speed $v_d \sim \varepsilon^{-3/2}$ is very large, so the last assumption $v < v_d$ in (28) is unlikely to be violated. Note that the condition $v < v_d$ can be violated if the oil saturation in the initial reservoir is lower than 1. If this happens, the saturation discontinuity becomes a part of the LTO wave.

4.4 Geometrical interpretation

We see that the resonance point provides extra conditions needed to determine the LTO wave parameters. To see that this is a generic phenomenon for systems of balance laws, we will provide a geometric interpretation for the LTO wave equations. It is convenient to choose θ, S, m and the fluxes of gaseous oil and oxygen denoted by $m_X = Xm$ and $m_Y = Ym$ as independent variables. The change of m_X and m_Y in the LTO wave is governed by ordinary differential equations (33), (34). The remaining variables θ, S, m are determined by equations (40), (42). Here the dependence $\theta = qm_Y/v$ and $m = 1 + m_X$ is linear. Thus, the essential variables are m_X, m_Y and S. Fig. 4(a) shows schematically the surface determined by the first equation in (40) relating S with m_X, m_Y. This surface has a fold. The fold line is given by condition (46), which corresponds to the vanishing derivative with respect to S taken from the left-hand side of (40). The fold projection determines a boundary of the feasible domain on the (m_X, m_Y)-plane, Fig. 4(a).

The constant state behind the LTO wave corresponds to $S = m_X = 0$, $m_Y = Y_{inj}$, and belongs to the lower part of the S-surface in Fig. 4(a). The constant state S_0, $mX = X_0m_0$ and $m_Y = 0$ ahead of the LTO wave belongs to the upper part of the S-surface. These two states are denoted by L and R in Fig. 4. Thus, the LTO wave profile must be an integral curve that passes from the lower to the upper part of the S-surface. When ξ varies, the typical integral curve reaches the resonance line (fold) at some finite value of ξ as shown in Fig. 4. It cannot be extended outside the feasible domain on the (m_X, m_Y)-plane, neither pass to the other side of the S-surface. However, there can be special integral curves passing through a singular point r

on the resonance line. This singular point corresponds to the intersection of integral curves on the S-surface, i.e., their tangency at the point r on the (m_X, m_Y)-plane, Fig. 4(a,b). Thus, the LTO wave profile can be constructed if the parameters are chosen to ensure that both constant states of the LTO wave (L and R) lie on such a special curve, as shown in Fig. 4(b). This provides an extra restriction on the wave parameters.

Let us see how this restriction gives the LTO wave solution under the assumption that the vaporization rate w_v in (33) is very high. In this case the integral curves on the (m_X, m_Y)-plane are approximately parallel to the m_X-axis and lead to the equilibrium points $X_{eq}(\theta)$, as shown in Fig. 4(c) (the integral curves on both sides of the S-surface coincide when projected). The set of equilibrium points is shown by the bold line. It is also an approximate integral curve with direction corresponding to decreasing m_Y, as determined by (34). The unique way to construct the LTO wave profile is presented in Fig. 4(c). The first part of the profile is parallel to the m_X-axis. Is starts at the point L and determines the vaporization region in Fig. 3. The second part of the profile is the equilibrium curve determining the reaction region. It ends at the point R. The two parts are connected at the resonance point on the fold line.

The general mathematical theory for traveling waves in systems of balance laws [6] predicts the possibility of singularities in the wave profile. Singularities occur when the matrix of coefficients of the derivative terms in system (31)–(35) becomes singular at some state inside the wave. Our approach shows how this singularity can be resolved in order to find extra determining conditions. The following conditions for the resonance point separating the vaporization and reaction regions are the main result

$$X_r = X_{eq}(\theta_r), \quad v = (\partial F/\partial S)_r. \tag{51}$$

The distinctive feature of our problem is that conditions (51) are independent on specific forms of vaporization and reaction rates. All we need to know is that vaporization is much faster than the LTO reaction. Also one can verify that condition (51) does not require the simplifications made in the derivation of wave equations in the beginning of this section.

The resonance condition (51) has a simple physical explanation. The oil saturation undergoes a finite change in a very thin vaporization region. Thus, this region must propagate with characteristic speed $\partial F/\partial S$ (singularities propagate along characteristic lines in hyperbolic systems of PDE's). This characteristic speed can be evaluated at the boundary between the vaporization and reaction regions, where $X = X_{eq}(\theta)$.

5 Effects of diffusion, capillary pressure and heat losses

The thermal conduction is described by a term $\lambda \partial^2 T/\partial x^2$ added to the right-hand side of (9), where λ [W/mK] is the thermal conductivity of the porous medium. One can see that taking into account only thermal conductivity (without other diffusion terms) does not change LTO wave parameters. The reason is that the heat conduction term has no influence on the form of the S-surface in the (m_X, m_Y, S) space and, thus, the resonance condition (51) remains unchanged.

The gas mass diffusion can be modelled by the term $\frac{\partial}{\partial x}\left(D(1-S)\frac{\partial X}{\partial x}\right)$ added to the right-hand side of (3), where D [m^2/s] is the diffusion coefficient. Similar terms appear in (4), (5). The diffusion terms become important when the gas composition changes essentially in the distance of order $L_D = D\varphi/u_{inj}$ [m], where u_{inj}/φ is the gas speed at injection point.

The dominant second order derivative term in the liquid oil balance equation (2) is related to capillary effects. The magnitude of this term is characterized by the quantity $D_S = \sqrt{\kappa\varphi}(\gamma/\mu_o)\cos\Theta$ [m^2/s], where κ [m^2] is the rock permeability, γ [N/m] is the liquid oil surface tension and Θ is the contact angle (see, e.g., [1]). Capillary effects become important when the oil saturation S changes essentially in the distance of order $L_S = D_S/v$ [m], a formula that relies on the fact that the oil speed is close to the LTO wave speed v.

parameter	meaning	value
Q_c	LTO reaction enthalpy	390 kJ/mole of O_2
Q_v	vaporization heat	34 kJ/mole of oil
R	ideal gas constant	8.314 J/mol K
C_m	heat capacity of porous medium	2×10^6 J/m^{3}K
c_g	heat capacity of gas	$3.5R$ J/mol K
c_o/M_o	heat capacity of oil	2.1 kJ/kg K
T_{res}	reservoir temperature	323 K (50°C)
T_{bn}	normal boiling temperature of oil	373 K (100°C)
Y_{inj}	molar fraction of oxygen in air	0.21
$M_o\rho_o$	oil density	900 kg/m^3
M_o	average molar mass of oil	0.1 kg/mole
φ	porosity	0.3

Table 1: Nomenclature, units and typical values of reservoir parameters.

When diffusion terms are taken into account, the LTO wave solution will be changed in a thin vaporization region and in the region near the resonance point, where the derivative $\partial S/\partial x$ becomes infinite. However, the resonance condition (determining the LTO wave parameters) remains approximately valid, if the diffusion terms are small in the reaction region. Recall that this condition is related to impossibility of extending the wave solution through the resonance point. The appropriate length scale in the reaction region is determined as $L = Y_{inj}\rho_g^* u_{inj}/W_c^{max}$ [m], where $Y_{inj}\rho_g^* u_{inj}$ is the injected oxygen flux and W_c^{max} [mole/m^{3}s] denotes the LTO reaction rate at the highest temperature. Thus, the gas mass diffusion and capillary effects can be neglected when $L \gg \max(L_D, L_S)$. One can check that L is proportional, and L_D, L_C are inversely proportional to the injected gas speed u_{inj}. Thus, diffusion effects are small when u_{inj} is high enough, as one could expect.

Our analysis of the LTO wave is valid when the lateral heat losses in the wave are much smaller than the heat generated by LTO. Estimating the rate of lateral heat losses for a reservoir of width h [m] as $\lambda(\partial T/\partial y) \sim \lambda T^*/h$ and the heat generation rate as $T^* C_m v h$, we obtain the condition

$$h^2 \gg \lambda/(C_m v), \tag{52}$$

where v [m/s] is the dimensional wave speed. Thus, heat losses in the LTO wave can be neglected if the reservoir width is large. A typical value of the right-hand side in (52) is 1 m^2. Heat losses in the hot zone upstream of the LTO wave lead to slow temperature decrease to the reservoir temperature, $T \to T_{res}$. This process, however, has minor influence on the LTO wave parameters.

6 Analysis of LTO waves for typical reservoir parameters

Typical values of reservoir parameters are given in Table 1. The quadratic model $k_o = S^2$, $k_g = (1-S)^2$ for relative permeabilities yields $\psi(S) = S^2/(1-S)^2$. We approximate the air and oil viscosities as $\mu_g = 1.8 \times 10^{-5}\sqrt{T/293\,[K]}$ and $\mu_o = 4 \times 10^{-10}\rho_o \exp(3.8\,T_b/T)$ [Pa s], see [2].

Consider the case with total pressure $P_{tot} = 10^6$ [Pa] (10 atm). Using (10), we compute the boiling temperature $T_b = 472$ [K]. Then we use (12), (18) to compute the temperature scale $T^* = 149$ [K] and the dimensionless parameters $\varepsilon = 0.02$, $b = 2.04$, $q = 7.19$, $h_v = 27.4$. Solving numerically system (49), we find $S_r = 0.202$, $\theta_r = 0.455$. Thus, the temperature behind the LTO wave equals $T_r = T_{res} + T^*\theta_r = 391$ [K]. Using (12), (43), we obtain the LTO wave speed as $v = 0.22\,u_{inj}$. The oil saturation downstream of the LTO wave is found using (50) as $S_0 = 0.576$.

Fig. 5 shows the LTO wave parameters for the pressure P_{tot} changing between 1 and 50 [atm].

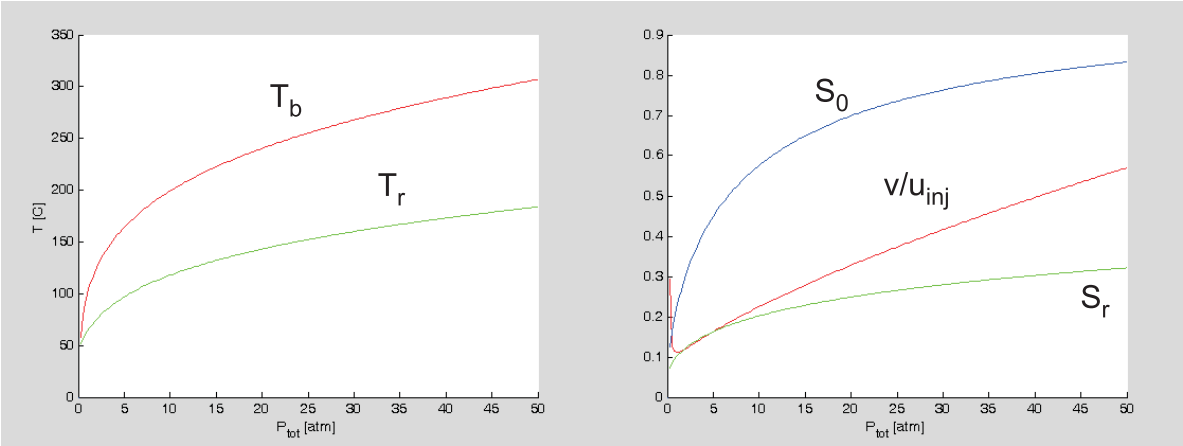

Figure 5: The oil boiling temperature T_b, the temperature T_r upstream of the LTO wave, the LTO wave speed v relative to the injection speed u_{inj}, and the saturations S_0 and S_r ahead of the LTO wave and at the resonance point depending on the reservoir pressure P_{tot}.

The oil saturation S_0 ahead of the wave increases rapidly up to the value 0.5 at the pressure $P_{tot} = 7\,[\text{atm}]$, and then increases slower up to values over 0.8. The dependence of the LTO wave speed on pressure is approximately linear. It reaches the value of one half of the gas Darcy velocity at $P_{tot} = 40\,[\text{atm}]$. Computations show that only a small part of oil vaporizes or reacts. As a result, the oil velocity uf_o/φ downstream of the LTO wave computed using (8) appears to be close to the LTO wave speed v. Thus, the LTO wave represents a mechanism of complete oil displacement by means of temperature increase inside the LTO wave, which leads to decrease of oil viscosity and increase of gas flux in the wave.

The spatial distribution of dependent variables in the LTO wave is determined by the LTO rate W_c. Experimental studies [4, 5] show large variation of LTO reaction rates that may differ about hundred times for different types of oil. Let us consider the reaction rate W_c [moles of $O_2/\text{m}^3\text{s}$] that agrees with the results of [5] as

$$W_c = 3.1 \times 10^6 S \exp\left(-\frac{7066}{T[\text{K}]}\right)\left(\frac{Y P_{tot}}{P_{atm}}\right)^{0.5}. \tag{53}$$

Consider the same pressure as above, $P_{tot} = 10^6\,[\text{Pa}]$ (10 atm). The characteristic length of the LTO wave is found from (12) as $x^* = 1.1 \times 10^5 u_{inj}$ [m], where we used $Y = Y_{inj}$, $S = 0.5$ and $T = T_{res}$ in (53). The coefficient $1.1 \times 10^5\,[\text{s}] \sim 1\,\text{day}$ characterizes the time necessary for self-ignition of the LTO wave.

The length L characterizing the LTO reaction at the highest temperature $T_r = 390\,[\text{K}]$ is found similarly as $L = 2.46 \times 10^3 u_{inj}$ [m]. Taking the typical values of gas diffusion coefficient $D = 2 \times 10^{-5}\,[\text{m}^2/\text{s}]$ and the capillary effect parameter as $D_S = 10^{-5}\,[\text{m}^2/\text{s}]$, we estimate the corresponding characteristic lengths as $L_D = D\varphi/u_{inj} = 6 \times 10^{-6}/u_{inj}\,[\text{m}]$ and $L_S = D_S/v = 4.5 \times 10^{-5}/u_{inj}\,[\text{m}]$. For the injection velocity $u_{inj} = 10^{-3}\,[\text{m/s}]$ (86 [m/day]) we have $L = 2.46\,[\text{m}] \gg \max\{L_D, L_S\} = 0.045\,[\text{m}]$, so the diffusion effects are small. Note that experimental results for a different type of oil [4] gave almost 100 times lower reaction rates and, hence, for such oil diffusion effects can be neglected even for much lower injection speeds.

References

[1] P. Bedrikovetsky and G. Rowan. *Mathematical theory of oil and gas recovery: with applications to ex-USSR oil and gas fields.* Kluwer, 1993.

[2] R.B. Bird, W.E. Stewart, and E.N. Lightfoot. *Transport Phenomena*. Wiley, New York, 1960.

[3] J. Bruining, A. A. Mailybaev, and D. Marchesin. Filtration combustion in wet porous medium. *SIAM J. Appl. Math.*, 70:1157–1177, 2009.

[4] M. K. Dabbous and P. F. Fulton. Low-temperature-oxidation reaction kinetics and effects on the in-situ combustion process. *SPE Journal*, 14(3):253–262, 1974.

[5] N. P. Freitag and B. Verkoczy. Low-temperature oxidation of oils in terms of SARA fractions: why simple reaction models don't work. *Journal of Canadian Petroleum Technology*, 44(3):54–61, 2005.

[6] A. G. Kulikovskii, N. V. Pogorelov, and A. Y. Semenov. *Mathematical Aspects of Numerical Solution of Hyperbolic Systems*. Chapman and Hall/CRC, Boca Raton, FL, 2001.